Journal of Nanomaterials & Molecular Nanotechnology

RESEARCH ARTICLE

Investigation of Structural and Optical Properties of Substituted MgFe$_2$O$_4$ Nanoferrites

Indu Sharma* Lalita Kumari

Abstract

Ferrite materials are one of the magnetic classes of materials, which have a variety of applications in the industry as well as in day-to-day life. In general, there are two broad categories of these materials i.e. soft and hard ferrites. These categories are based on the response of these materials in the magnetic field. In the present work, we aimed to work on the substituted soft spinel nano ferrites i.e. substituted Mg-Mn ferrite nanoparticles having space group Fd$_3$m-O$_7$. Mg-Mn ferrite nanoparticles have various applications in the industry owing to which they have been explored by many materials scientists for the last two decades. In fact, many researchers have studied the pure and substituted MgFe$_2$O$_4$ ferrites in bulk, nano form but no literature is available on the investigation of Cd^{3+}, and La^{3+} substituted MgFe$_2$O$_4$ nano ferrites synthesized via sol-gel technique. Therefore, in the present work, we have planned to study the effects of Cd^{3+} and La^{3+} doping on the structural and optical properties of MgFe$_2$O$_4$ nano ferrites.

Keywords

Mg Nanoferrites; XRD; SEM; TEM; UIV-Vis Spectroscopy

Introduction

Spinel ferrites are very important because of their magnetic properties, high electrical resistivity and low eddy current and dielectric loss. The properties of these ferrites are only dependent upon their chemical composition, cation distribution, dopant and method used for preparation. The structure of the spinel crystal is determined by the oxygen ions lattice. The oxygen ions radius is several times larger than the radii of the metallic ions. In spinel, the smallest cell contains eight molecules of MeFe$_2$O$_4$ where, Me is divalent metal ions (Me=Cd^{2+}, Ni^{2+}, Cu^{2+}, Zn^{2+}, Co^{2+}). Large oxygen ions form an FCC lattice. In the cubic close packing, there are two interstitial sites, the first one is a tetrahedral site (A) and the second is an octahedral site (B), where the tetrahedral site is surrounded by 4 oxygen ions and the octahedral site is surrounded by 6 oxygen ions. In this cubic unit cell, there are 64 tetrahedral sites and 32 octahedral sites are present of which only 8 and 16 respectively, are occupied by metal ions. In a tetrahedral site, there is vacant space between the four

atoms in which three atoms touch each other in a plane and the fourth atom lies in the symmetrical position on top. So tetrahedral site has a defined geometry and having space for the incoming atom (dopant). In an octahedral site, there is vacant space between six regular atoms that form an octahedron. In this case, four regular atoms are present in a plan while the other two are in a symmetrical position just above or below [1]. The ferrites with garnet structure have general formula Ln$_3$Fe$_5$O$_{12}$. Dodecahedral (eightfold), Octahedral (sixfold) and Tetrahedral (fourfold) are three different types of interstitial sites. Comparatively, dodecahedral sites occupy a large size and rare-earth ions. The Fe^{3+} ions are distributed on both other sites.

A garnet unit cell consisting of 8 formula units is similar to spinel ferrites. A unit cell is consisting of 16 dodecahedral, 16 octahedral and 24 tetrahedral sites. One formula unit of garnet ferrites can be expressed as $3M_2O_{35}Fe_2O_3$. Where $3M_2O_3$ occupy the dodecahedral site, $3Fe_2O_3$ occupy the tetrahedral site and $2Fe_2O_3$ occupy the octahedral site [2,3]. M-type hexaferrite has the same structure as natural mineral magnetoplumbite [4] and the generic formula can be represented as MFe$_{12}$O$_{19}$. In the said formula M can be the divalent ions Ba^{2+}, Sr^{2+}, or Pb^{2+}. There are two blocks S and S*. The magnetoplumbite structure contains oxygen layers and is connected by block R containing barium or strontium ion. The barium-containing layer is hexagonally packed with respect to the two oxygen layers and between those barium ions, containing layer is cubically packed with respect to the four oxygen layers. The basal plane containing the barium ion is a mirror plane of the R block and consequently, the block preceding and succeeding the R block must be rotated over 180° with respect to each other. One molecule layer is consists of five oxygen layers and further one unit cell is made of two molecules. The crystallographic structure can be described as RSR*S* and the space group is denoted as P6$_3$/mmc (D$^4_{6h}$) [5]. In a hexagonal structure on 11 different symmetry sites, the M-type hexaferrite crystallizes have 64 ions per unit cell. Hexaferrite is showing the different Fe sites with their surroundings. There are 38 oxygen ions, 24 ferric ions and 2 Me ions (Me=Ba^{2+}, Sr^{2+}, Pb^{2+} and La^{3+}) in the unit cell. The 24 ferric ions are distributed over five distinct sites i.e. 2a, 2b, 4f$_1$, 4f$_2$ and 12k. Out of these five sites 2a, 4f$_2$ and 12k are octahedral, 4f$_1$ is tetrahedral and 2b site is surrounded by five oxygen atoms forming a trigonal bipyramid. The oxygen ions occupy 4e, 4f, 6h and 12k sites forming a closed pack lattice. The fourth type of ferrites is known as orthoferrites. The formula for orthoferrites component is RFeO$_3$, in which R represents rare earth or transition metal. They have ABO form perovskite structure, in which A is a twelve-coordinated oxygen site and is occupied by magnetic ions of lanthanide (rare earth) series; B usually occupies a transition metal ion Fe^{3+}. An ideal perovskite structure is simply cubic. At room temperature, the mineral perovskite (CaTiO$_3$) is known to be orthorhombic and when the temperature is increased above 9000C then becomes cubic. Other ceramics with the perovskite structure include BaTiO$_3$, SrTiO$_3$, and KNbO$_3$. The unique magneto-optical properties of orthoferrites are a direct consequence of their structure. The domain of orthoferrites is that their unit cell is slightly orthorhombic instead of cubic like BaTiO$_3$. In fact, the structure of the orthoferrites unit cell is close to being cubic, but to some extent, the angle between the c-axis and the a-b plane is greater than 90°. This orthorhombic cell manifests itself as a slight canting in the unit cell of the orthoferrites usually in the

*Corresponding author: Indu Sharma, Department of Physics, Career Point University, Hamirpur, Himachal Pradesh, India, Telephone: +91 9418469600; E-mail: indu.phy@cpuh.in

order of 0.6° [6]. An example of a common orthoferrites is $YFeO_3$. It crystallizes orthorhombic unit cells with distorted perovskite structures. The distortion in the ideal perovskite is mainly due to the position of the yttrium ions, whereas the Fe^{3+} ions exist in an octahedral environment. This structure can be imagined as a three-dimensional network of strings of FeO_6 octahedral. One of the anions (O^{2-}) forms the common apex of the two adjacent octahedral and displays the super-exchange bond (Fe-O-Fe) between two iron ions.

Generally, there are two types of magnetic interactions:

(i) Direct exchange interaction

(ii) Super-exchange interaction

The direct exchange interaction takes place due to an overlap of orbital of two interacting magnetic ions. The importance of this interaction is only when the separation between the interacting magnetic ions is small enough to allow overlap. In spinels, the separation between the cations is large having no overlap of the orbital of the magnetic ion. So, in spinel instead of direct exchange, the exchange interaction takes place by the participation of oxygen anions and which is known as super-exchange interaction. Since in ferrites, magnetic ions occupy (A) and (B) sites, so there are three possible super-exchange interactions (A-A), (B-B), and (A-B). A-B interaction heavily predominates over A-A and B-B interactions. A-B interaction aligns all magnetic spins at A-site in one direction and B-site in opposite direction thus constitutes two saturated and magnetized sub-lattices at 0 K. The net magnetization of the lattice is the difference of magnetization of B and A sub-lattices. In M-type hexagonal ferrites, the M ions (Me=Ba, Sr, Pb and La) occupy 2d sites. The arrangement of 12 Fe^{3+} is as 6 Fe^{3+} are in 12k site having up spin, 2 ions in $4f_2$ and $4f_1$ having down spin and 1 ion in 2a and 2b site having up spin. The above arrangement is made to facilitate 8 Fe^{3+} in the upward direction and 4 in the downward direction. So that 4 upward and downward can cancel each other and the net moment is obtained of 4 Fe^{3+} per formula unit. As per Fe^{3+} configuration, there are 5 unpaired electrons in 3d orbital and each Fe^{3+} ion has the magnetic moment of 5 μB. The total moment is 20 μB per formula unit S.I. Ahmad et al. have synthesized $MgCe_xFe_{2-x}O_4$ nano ferrites via sol-gel auto combustion method and reported the structural, FTIR, and XPS study [7]. D Chen, et al. have prepared magnesium ferrite nanoparticles by microwave-assisted ball milling method and reported the magnetic properties of the same [8]. V Sepelak, et al. have synthesized $MgFe_2O_4$ nano ferrites by high energy milling method and reported the magnetic and Mössbauer properties [9]. P Reddy, et al. have synthesized $MgFe_2O_4$ ferrite by spark plasma sintering method and reported the influence of temperature on the structural and magnetic properties [10]. A Pradeep, et al. have synthesized $MgFe_2O_4$ nano ferrites by sol-gel method and reported the structural, FTIR and magnetic properties [11]. NM Deraz et al. have reported the structural and magnetic properties of $Zn_{0.5}Mg_{0.5}Fe_2O_4$ ferrite [12].

SD Chhaya, et al. have reported the structural, electrical and magnetic properties of calcium doped magnesium ferrite [13]. KK Bamzai, et al. have synthesized $MgCa_xFe_{2-x}O_4$ ferrite by ceramic method and reported the structural and magnetic properties [14]. V Naidu, et al. have reported the electrical and magnetic properties of Ce-Gd substituted Magnesium ferrite [15]. HS O'Neill, et al. have reported the influence of temperature on the cation distribution of magnesium ferrite [16]. ED Grave, et al. have reported the Mössbauer properties of $MgFe_2O_4$ ferrites and evolved the cation distribution from Mössbauer method [17]. RG Kulkarni et al. have reported the

Mössbauer spectroscopic study of zinc substituted magnesium ferrite [18]. Owing to the various applications of Mg-Mn ferrites, many researchers have investigated the properties of these materials by doping by different ions as well as by doping by different techniques for synthesis. In fact, many researchers have studied the pure and substituted $MgFe_2O_4$ ferrites in bulk, nano form but no literature is available on the investigation of Cd^{3+}, and La^{3+} substituted $MgFe_2O_4$ nano ferrites synthesized via sol-gel technique. Therefore, in the present work, we have investigated the effects of Cd^{3+} and La^{3+} doping on the structural and optical properties of $MgFe_2O_4$ nano ferrites.

Experimental

The samples were prepared *via* the sol-gel method [19,20]. The sol-gel method has provided a very important means of preparing inorganic oxides. It is a wet chemical method and multistep process involving both chemical and physical processes. In this method, the metal precursors are in form of nitrates dissolved in distilled water and citric acid ($C_6H_8O_7$) is used as fuel. Cadmium doped magnesium nano ferrite series with generic formula $Mg_{1-y}Cd_yLa_xFe_{2-x}O_4$ (x=0.0, 0.1, y=0.1, 0.2) were synthesized using AR graded nitrates of the constituent elements. The chemicals used in the synthesis procedure were ferric nitrate, magnesium nitrate, cadmium nitrate, lanthanum nitrate, citric acid, ethylene glycol, and ammonia solution, which was used to maintain pH. In a stoichiometric ratio, ferric nitrate, magnesium nitrate, cadmium nitrate and lanthanum nitrate were dissolved in 50 ml distilled water to obtain a mixed solution and on the other side, citric acid in a stoichiometric ratio with nitrates was dissolved in 50 ml distilled water. Both the solutions were kept on a magnetic stirrer to obtain a clear solution, then the nitrates were added to the citric acid solution, and the solution was then heated on a hot plate magnetic stirrer with constant stirring at room temperature for 2 hours. Then ammonia solution was added to maintain the pH at 7 of the solution, and then ethylene glycol in the corresponding stoichiometric ratio with nitrates and citric acid was added to the solution and the solution was heated at 80°C and was continuously stirred. After 4 hours-5 hours, the liquid solution was converted into a gel and then was kept at a high temperature for conversion into ash. After that resultant ash form was cooled and was crushed to obtain its powdered form. The prepared powder was sintered at 400°C for 4 hours.

Result and Discussion

Structural study

The XRD patterns of $Mg_{1-y}Cd_yLa_xFe_{2-x}O_4$ ferrite particles are illustrated in figure 1. The diffraction peaks are at (220), (311), (400), (422), (511), (440) are observed which are found to be matching well with the JCPDS card no-17-0464, therefore, anticipates the development of spinel-cubic configuration with space group Fd3m-Oh[7] [21,22].

The particle size of the prepared ferrites was estimated by employing the following Debye-Scherrer formula [23]:

$$D = \frac{0.9\lambda}{\beta \cos\theta} \qquad (1)$$

Where 'D' is the particle size, 'β' is the full width at half maximum (FWHM) of the (311) peak, 'λ' is the X-ray wavelength (1.54 Å) and 'θ' is the angle of diffraction. The lattice parameter (a) of the nano ferrite was calculated by using the following relation [24]:

$$D = \frac{\lambda}{2\sin\theta}\sqrt{h^2 + k^2 + l^2} \qquad (2)$$

Theroux-ray density and hopping length at the A and B site is estimated by employing the following relations [25,26]:

$$\rho_{x-ray} = \frac{8M}{Na^3} \qquad (3)$$

$$L_A = \frac{a\sqrt{3}}{4} \qquad (4)$$

$$L_B = \frac{a\sqrt{2}}{4} \qquad (5)$$

Where the symbols have their usual meanings. The estimated values of the particle size, lattice parameter, x-ray density and hopping lengths are given in Table 1.

Table 1: Values of the particle size, lattice parameter, x-ray density and hopping lengths.

Sample	Particle size (nm)	Lattice parameter (Å)	X-ray density (g/cm³)	LA (Å)	LB (Å)
$Mg_{0.9}Cd_{0.1}Fe_2O_4$	18.09	8.38	4.7	3.631	2.965
$Mg_{0.8}Cd_{0.2}La_{0.1}Fe_{1.9}O_4$	12.71	8.39	5.07	3.634	2.967
$Mg_{0.7}Cd_{0.3}La_{0.2}Fe_{1.8}O_4$	10.09	8.45	5.35	3.659	2.987

The particle size was observed to decrease while the lattice parameter was observed to increase with the increase in dopants. The observed increase in the lattice parameter is owing to the difference in the ionic radius of the involved cations. The hopping lengths were observed to follow the same behaviour as observed for the lattice parameter. The observed behaviour of x-ray density suggested that with the increase in dopants the material is becoming denser. Figure 2 illustrates the scanning electron micrographs for $Mg_{1-y}Cd_yLaxFe_{2-x}O_4$ nano ferrite.
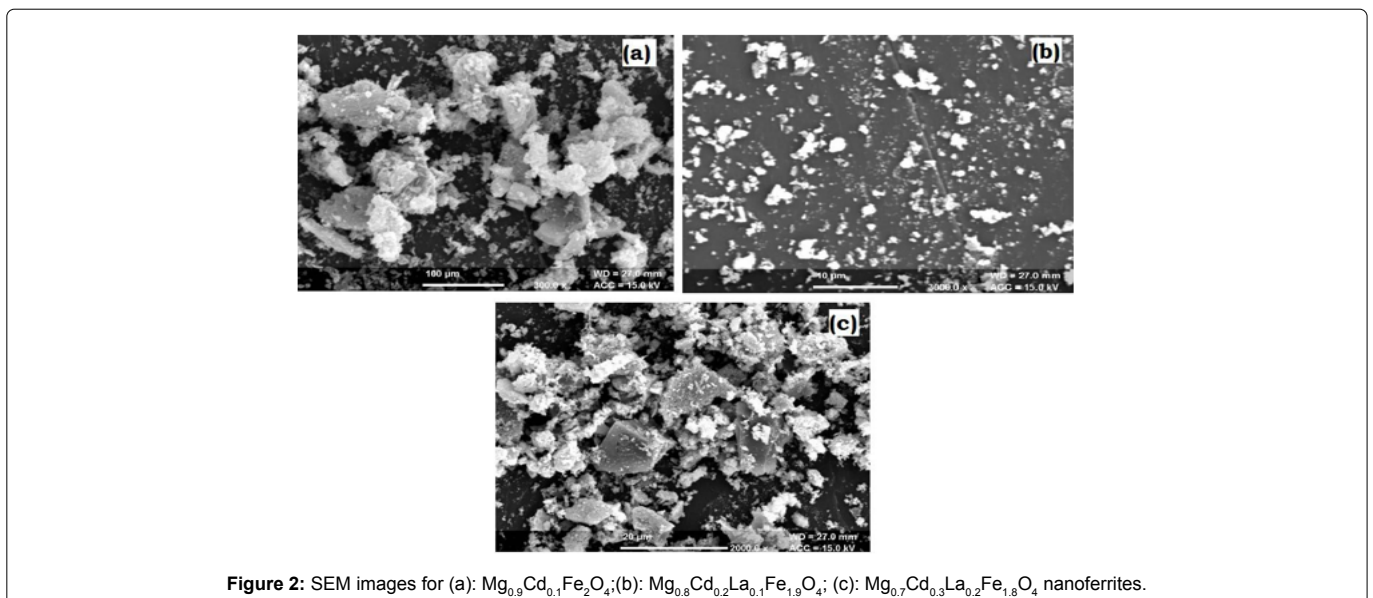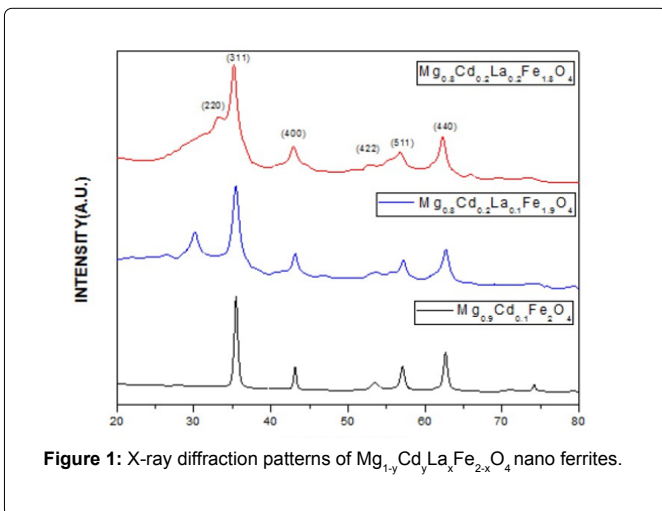
The SEM images are observed to have dispersed grains and the results are in agreement with the XRD study. Figure 3 illustrates the transmission electron microscopy images for $Mg_{1-y}Cd_yLa_xFe_{2-x}O_4$ nano ferrites. Again, the particle size as observed in the TEM results is in agreement with the XRD study for the synthesized nano ferrites.

Optical study

The bandgap is a significant parameter that gives information about the electrical conductivity of the ferrites. It represents the energy needed to move an electron to the conduction band from the valence band where the electron can participate in the conduction process. In the present work, the bandgap is estimated by considering a direct transition in between the conduction band and edges of the valence band with the help of the following relation [27]:

$$(\alpha h\nu)^2 = A(h\nu - E_g)^m \qquad (6)$$

Where α represents the absorption coefficient, A represents the

Figure 1: X-ray diffraction patterns of $Mg_{1-y}Cd_yLa_xFe_{2-x}O_4$ nano ferrites.

Figure 2: SEM images for (a): $Mg_{0.9}Cd_{0.1}Fe_2O_4$;(b): $Mg_{0.8}Cd_{0.2}La_{0.1}Fe_{1.9}O_4$; (c): $Mg_{0.7}Cd_{0.3}La_{0.2}Fe_{1.8}O_4$ nanoferrites.
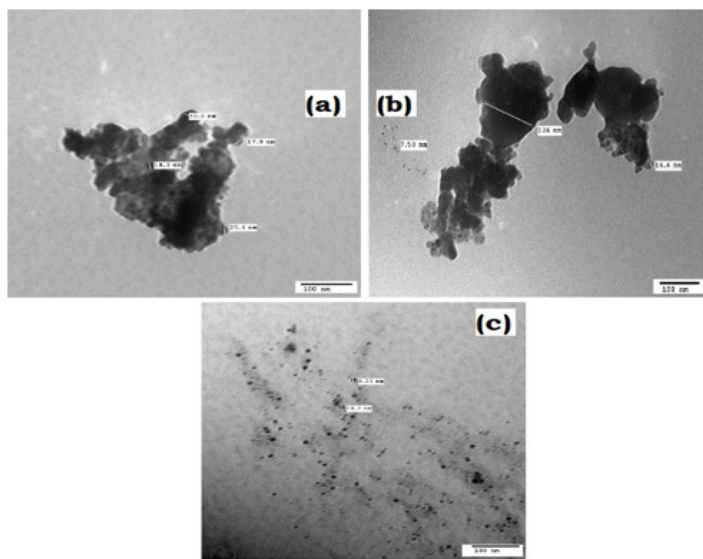
Figure 3: TEM images for (a): $Mg_{0.9}Cd_{0.1}Fe_2O_4$; (b): $Mg_{0.8}Cd_{0.2}La_{0.1}Fe_{1.9}O_4$; (c): $Mg_{0.7}Cd_{0.3}La_{0.2}Fe_{1.8}O_4$ nanoferrites.
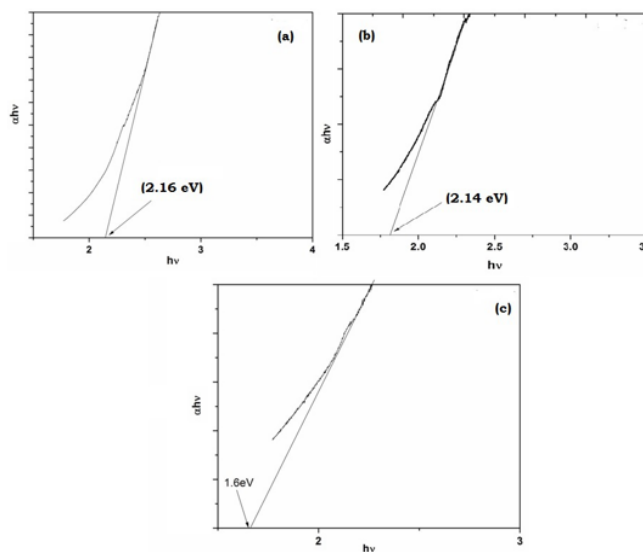

Figure 4: UIV-Vis spectra for (a): $Mg_{0.9}Cd_{0.1}Fe_2O_4$; (b): $Mg_{0.8}Cd_{0.2}La_{0.1}Fe_{1.9}O_4$; (c): $Mg_{0.7}Cd_{0.3}La_{0.2}Fe_{1.8}O_4$ nanoferrites.

edge width parameter, Eg represents the energy band gap and m is the constant dependent degree of transition having value 2 for direct optical band gap while has value ½ for indirect optical bandgap.

Figure 4 represent the Tauc plots of (a) $Mg_{0.9}Cd_{0.1}Fe_2O_4$ (b) $Mg_{0.8}Cd_{0.2}La_{0.1}Fe_{1.9}O_4$ (c) $Mg_{0.7}Cd_{0.3}La_{0.2}Fe_{1.8}O_4$ nano ferrites. The bandgap was observed to decrease (2.16-1.6 eV) with the increase in dopant. The decrease in bandgap can be owing to the doping of magnetic ions.

Conclusion

In the present work, we have planned to study the effects of Cd^{3+} and La^{3+} doping on the structural and optical properties of $MgFe_2O_4$

nano ferrites. The main findings drawn from the present work are summarized as below:

- The cadmium doped magnesium nanoferrite series with generic formula $Mg_{1-y}Cd_yLa_xFe_{2-x}O_4$ (x=0.0, 0.1, y=0.1, 0.2) were synthesized via sol-gel method.

- The XRD patterns of $Mg_{1-y}Cd_yLa_xFe_{2-x}O_4$ ferrite particles are found to be matching well with the JCPDS card no-17-0464, therefore, anticipated the development of spinel-cubic configuration with space group Fd_3m-Oh^7.

- The particle size was observed to decrease while the lattice parameter was observed to increase with the increase in dopants.

- The hopping lengths were observed to follow the same behaviour as observed for the lattice parameter.

- The SEM images were observed to have dispersed grains and the results were in agreement with the XRD study.

- The particle size as observed in the TEM results was found in agreement with the XRD study for the synthesized nano ferrites.

- The bandgap was observed to decrease (2.16-1.6 eV) with the increase in dopant.

References

1. Hashim M, Kumar S, Shirsath SE, Kotnala RK, Shah J, Kumar R (2013) Influence of Cr^{3+} ion on the structural, ac conductivity and magnetic properties of nanocrystalline Ni-Mg ferrite. Ceramics Int 39:1807-1819.

2. Pullar RC (2012) Hexagonal ferrites: A review of the synthesis, properties and applications of hexaferrite ceramics. Prog Mat Sci 57:1191-133.

3. Smit J, Wijn HPJ (1959) Ferrites. Philips Technical Library, Eindhoven, 150.

4. Dionne GF (2009) Magnetic oxides. New York: Springer 14:1-15.

5. Rösler S, Wartewig P, Langbein H (2003) Synthesis and characterization of hexagonal ferrites $BaFe_{12-2x}Zn_xTi_xO_{19}$ ($0 \leq x \leq 2$) by thermal decomposition of freeze-dried precursors. Crystal Res Tech J Experiment Industr Crystal 38: 927-934.

6. Schmool DS, Keller N, Guyot M, Krishnan R, Tessier M (1999) Magnetic and magneto-optic properties of orthoferrites thin films grown by pulsed-laser deposition. J App Phy 86: 5712-5717.

7. Ahmad SI, Kumar DR, Syed IA, Satar R, Ansari SA (2017) Structural, spectroscopic and magnetic study of nanocrystalline cerium-substituted magnesium ferrites. Arab J Sci Engg 42: 389-398.

8. Chen D, Zhang Y, Tu C (2012) Preparation of high saturation magnetic $MgFe_2O_4$ nanoparticles by microwave-assisted ball milling. Material Letter 82: 10-12.

9. Šepelák V, Baabe D, Mienert D, Litterst FJ, Becker KD (2003) Enhanced magnetization in nanocrystalline high-energy milled $MgFe_2O_4$. Scripta Materialia 48: 961-966.

10. Reddy MP, Shakoor RA, Mohamed AMA, Gupta M, Huang Q (2016) Effect of sintering temperature on the structural and magnetic properties of $MgFe_2O_4$ ceramics prepared by spark plasma sintering. Ceramics Int 42: 4221-4227.

11. Pradeep A, Priyadharsini P, Chandrasekaran G (2008) Sol-gel route of synthesis of nanoparticles of $MgFe_2O_4$ and XRD, FTIR and VSM study. J Magnet Magnetic Mat 320: 2774-2779.

12. Deraz N, Abd-Elkader OH (2015) Structural, morphological and magnetic properties of $Zn_{0.5}Mg_{0.5}Fe_2O_4$ as anticorrosion pigment. Int J Electrochem Sci 10: 7138-7146.

13. Chhaya SD, Pandya MP, Chhantbar MC, Modi KB, Baldha GJ, Joshi HH (2004) Study of substitution limit, structural, bulk magnetic and electrical properties of Ca^{2+} substituted magnesium ferrite. J Alloys Compounds 377: 155-161.

14. Bamzai KK, Kour G, Kaur B, Kulkarni SD (2014) Preparation, and structural and magnetic properties of Ca substituted magnesium ferrite with composition $MgCa_xFe_{2-x}O_4$ (=0.00, 0.01, 0.03, 0.05, 0.07). J Mat 2014: 1-10.

15. Naidu V, Sahib AK, Suganthi M, Prakash C (2011) Study of electrical and magnetic properties in nano-sized Ce-Gd doped magnesium ferrite. Int J Comput App 27: 40-45.

16. O'Neill HSC, Annersten H, Virgo D (1992) The temperature dependence of the cation distribution in magnesioferrite ($MgFe_2O_4$) from powder XRD structural refinements and Mössbauer spectroscopy. Am Mineral 77: 725-740.

17. De Grave E, Dauwe C, Govaert A, De Sitter J (1976) Cation distribution and magnetic exchange interactions in $MgFe_2O_4$ studied by the Mössbauer effect. Phy Stat Solidi 73: 527-532.

18. Kulkarni RG, Joshi HH (1985) The magnetic properties of the Mg-Zn ferrite system by Mössbauer spectroscopy. Solid Stat Commun 53: 1005-1008.

19. Chen DH, He XR (2001) Synthesis of nickel ferrite nanoparticles by sol-gel method. Mat Res Bullet 36: 1369-1377.

20. George T, Sunny AT, Varghese T (2015) Magnetic properties of cobalt ferrite nanoparticles synthesized by sol-gel method. In IOP Conference Series: Materials Science and Engineering. IOP Publishing 73: 012050.

21. Batoo KM, Raslan EH, Adil SF, Sharma I, Kumar G (2020) Investigation of electrical, magnetic, and optical properties of silver-substituted magnesium-manganese ferrite nanoparticles. J Mat Sci Mater Electron 20: 1-9.

22. Sharma A, Batoo KM, Raslan EH, Adil SF, Kumar G (2018) Structural and magnetic study of $Mn_{0.5}Zn_{0.5}Cu_xFe_{2-x}O_4$ nanoferrites synthesized *via* solution combustion method. Vacuum 157: 422-427.

23. Kumar G, Rani R, Sharma S, Batoo KM, Singh M (2013) Electric and dielectric study of cobalt substituted Mg-Mn nanoferrites synthesized by solution combustion technique. Ceramics Int 39: 4813-4818.

24. Kadam MR, Patil RP, Hankare PP (2012) Investigations on structural, electrical and magnetic properties of nickel substituted La-ferrites. Solid Stat Sci 14: 964-970.

25. Gupta M, Randhawa BS (2012) Microstructural, magnetic and electric properties of mixed Cs-Zn ferrites prepared by solution combustion method. Solid Stat Sci 14: 849-856.

26. Patil VG, Shirsath SE, More SD, Shukla SJ, Jadhav KM (2009) Effect of zinc substitution on structural and elastic properties of cobalt ferrite. J Alloys Compounds 488: 199-203.

27. Almessiere MA, Slimani Y, Korkmaz AD, Baykal A, Güngüneş H, Sözeri H, et al. (2019) Impact of La^{3+} and Y^{3+} ion substitutions on structural, magnetic and microwave properties of $Ni_{0.3}Cu_{0.3}Zn_{0.4}Fe_2O_4$ nanospinel ferrites synthesized via sonochemical route. RSC Advances 9: 30671-30684.

Author Affiliation *Top*

Department of Physics, Career Point University, Hamirpur, Himachal Pradesh, India